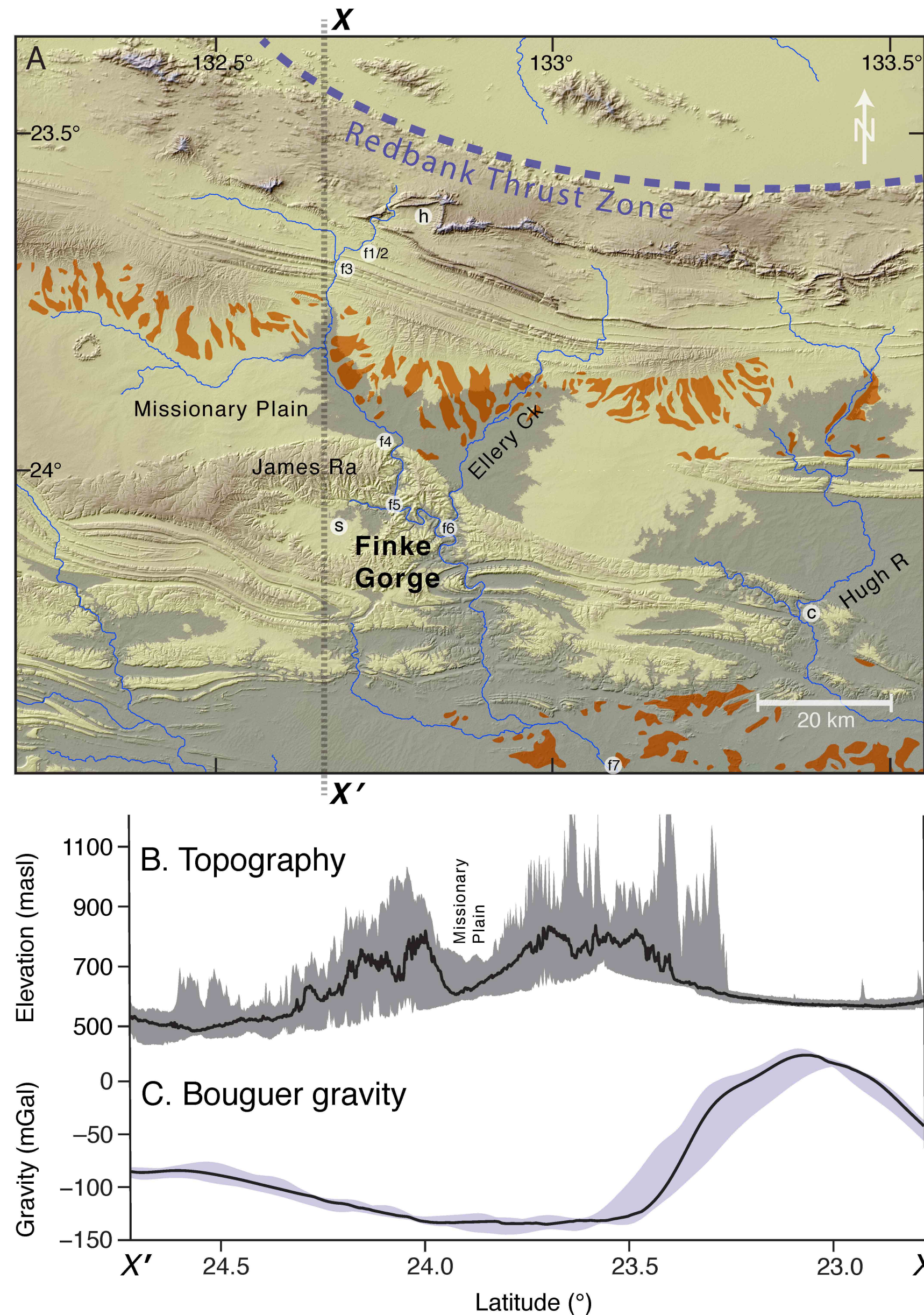


# Geomorphic imprints of dynamic topography & intraplate tectonism in central Australia



## The Finke Gorge enigma, central Australia

### Fig. 1. Central Ranges orogen and gravity anomaly.

(A) Topographic hillshade map (SRTM 1-arcsec data) of the Central Ranges centred on the upper Finke River (drainage area  $\sim 4500 \text{ km}^2$  upstream of the Ellery Creek junction) and Redbank Thrust Zone (purple dashes). The areas of low ( $< 614 \text{ masl}$ ) elevations (dark shading) illustrate the close topographic relationship between Finke's palaeovalley fill and the sediment-mantled pediments and terraces (orange) on Missionary Plain (Mabbutt, 1966; Raymond *et al.*, 2012). Note resistant ridges (h) marking the source of the Heavitree quartzite gravels; the synclinal basin (s) west of the gorge, containing a thin unconsolidated sediment cover; and a minor set of palaeovalley cutoffs (c) on the Hugh River. Locations of channel bed samples for  $^{10}\text{Be}$ - $^{26}\text{Al}$  analysis (f2–f4) are shown (see Fig. 3 for samples inside the gorge); note f7 is shown 22 km upstream of its true position.

(B) Topographic swath ( $X-X'$ :  $132.66 \pm 0.33^\circ$ ), showing maximum-minimum (grey band) and mean (black line) elevations.

(C) Bouguer gravity swath ( $X-X'$ :  $132.66 \pm 0.33^\circ$ ), showing maximum-minimum (purple band) and mean (black line) gravity.

# Extreme gravity lows ( $-150$ mGal) in central Australia

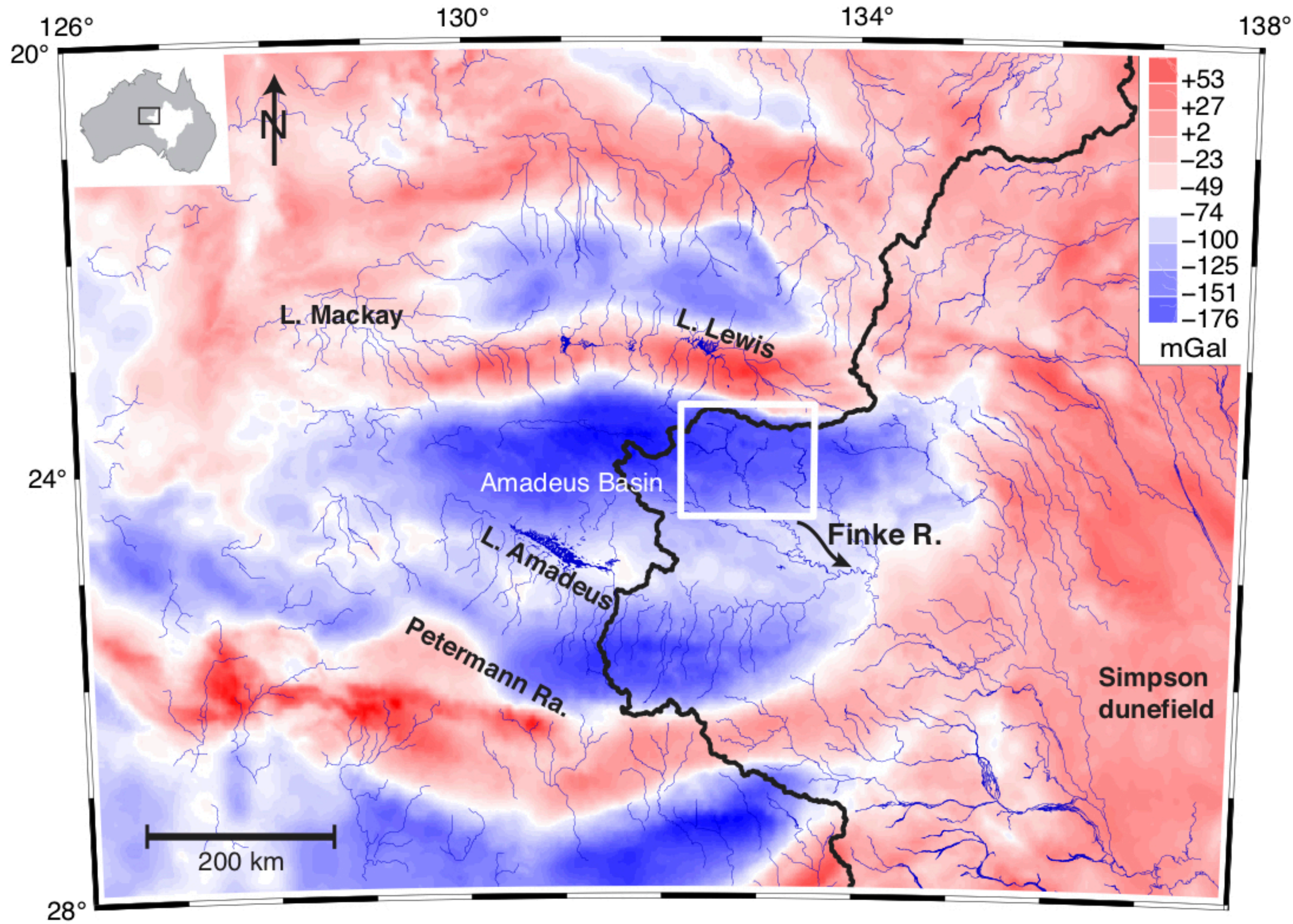


**Fig. 2. Gravity map of central Australia.**

A strong negative gravity anomaly (blue) is focused on the Central Ranges and surrounding area. The white box marks the area shown in Fig 1. The Redbank Thrust Zone corresponds with the northern margin of the Finke catchment, which itself defines the western part of the present-day LEB drainage divide (heavy black line). Note that (1) the western extent of the LEB connects the two most prominent gravity lows along the N- and S- margins of the Amadeus Basin from where the adjacent segments of the LEB divide divert eastward along steep gravity gradients; and (2) in this part of central Australia, rivers flow orthogonal to the gravity gradient—away from gravity troughs towards gravity ridges. Top-left inset shows Australia, the map area (black rectangle) and the 1.1 million km<sup>2</sup> LEB (white).

# Enigmatic intertwined gorges of the upper Finke River

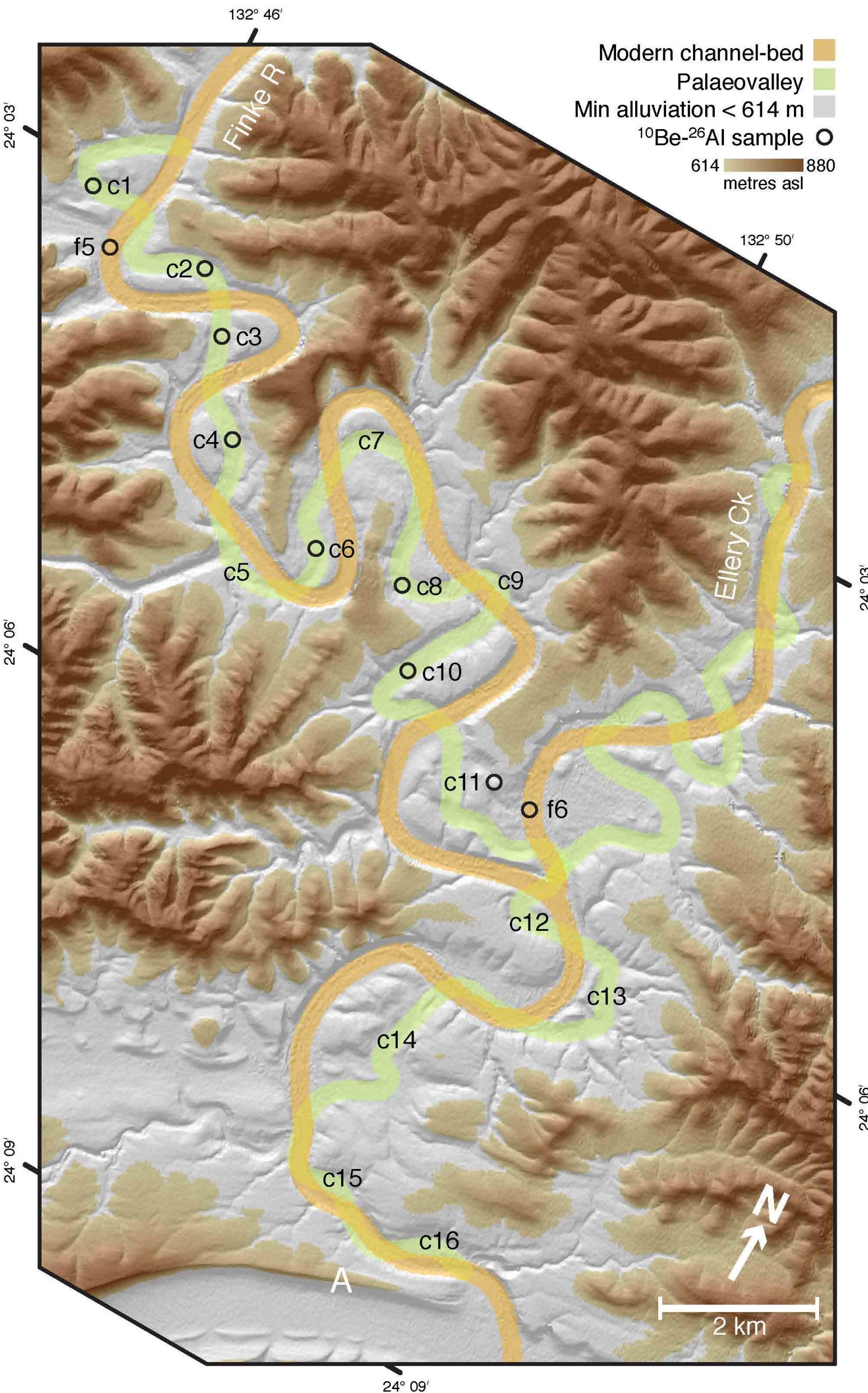


**Fig. 3. Intertwined epigenetic & palaeovalley gorges.**

The intertwined epigenetic (*Incision 2*) and palaeovalley (*Incision 1*) gorges of the Finke River and lower Ellery Creek (flow downpage) on a topographic hillshade map. Shown are the 16 palaeovalley cutoffs (c1–16) along the Finke and sites sampled for  $^{10}\text{Be}$ - $^{26}\text{Al}$  analysis (open circle), including the channel bed (f5, f6). Both channel sinuosity (2.15 in the modern gorge and 2.16 in the palaeovalley) and channel width are essentially equivalent for the two systems. Areas previously blanketed by sedimentary fill (grey shade), enabling lateral channel migration, are shown topping bedrock meander cores and shoulder surfaces (<614 m).

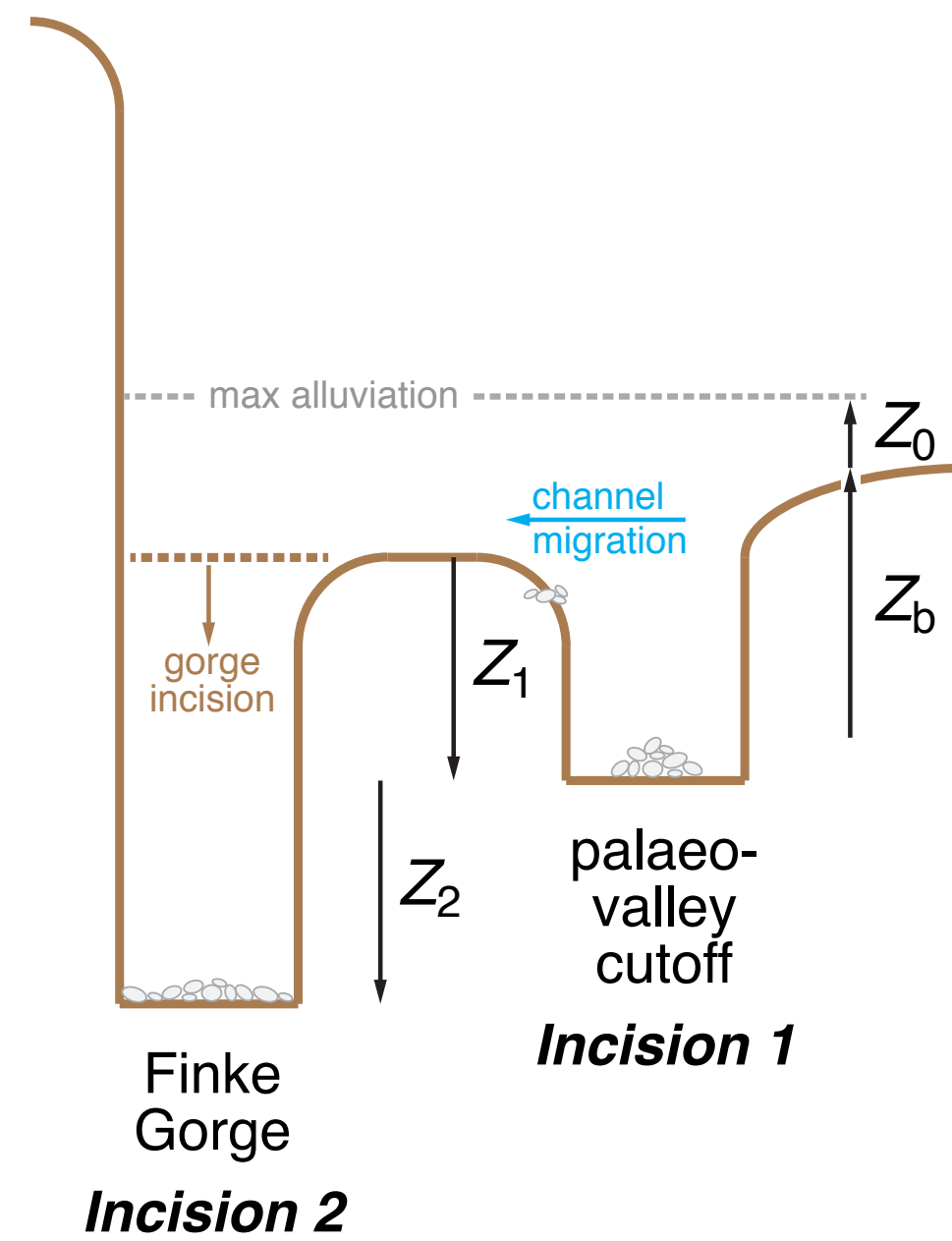


**Fig. 4. Schematic valley section.**

The Finke gorge (*Incision 2*) and palaeovalley (*Incision 1*) are shown here separated by a bedrock meander core of height,  $Z_1$ , which defines the minimum gravel-pile thickness to allow lateral channel migration. Samples for  $^{10}\text{Be}$ - $^{26}\text{Al}$  analysis were collected from gravel-pile crests in the palaeovalley at minimum burial depth,  $Z_b$ , below the extrapolated upper gravel surface (Figs. 3 and 5). To this minimum burial depth, is added an unknown sediment thickness,  $Z_0$ , of up to 20 m. All shown at ~10-times vertical exaggeration.

# MCMC inversion modelling of cosmogenic nuclide inventories in palaeovalley gravels

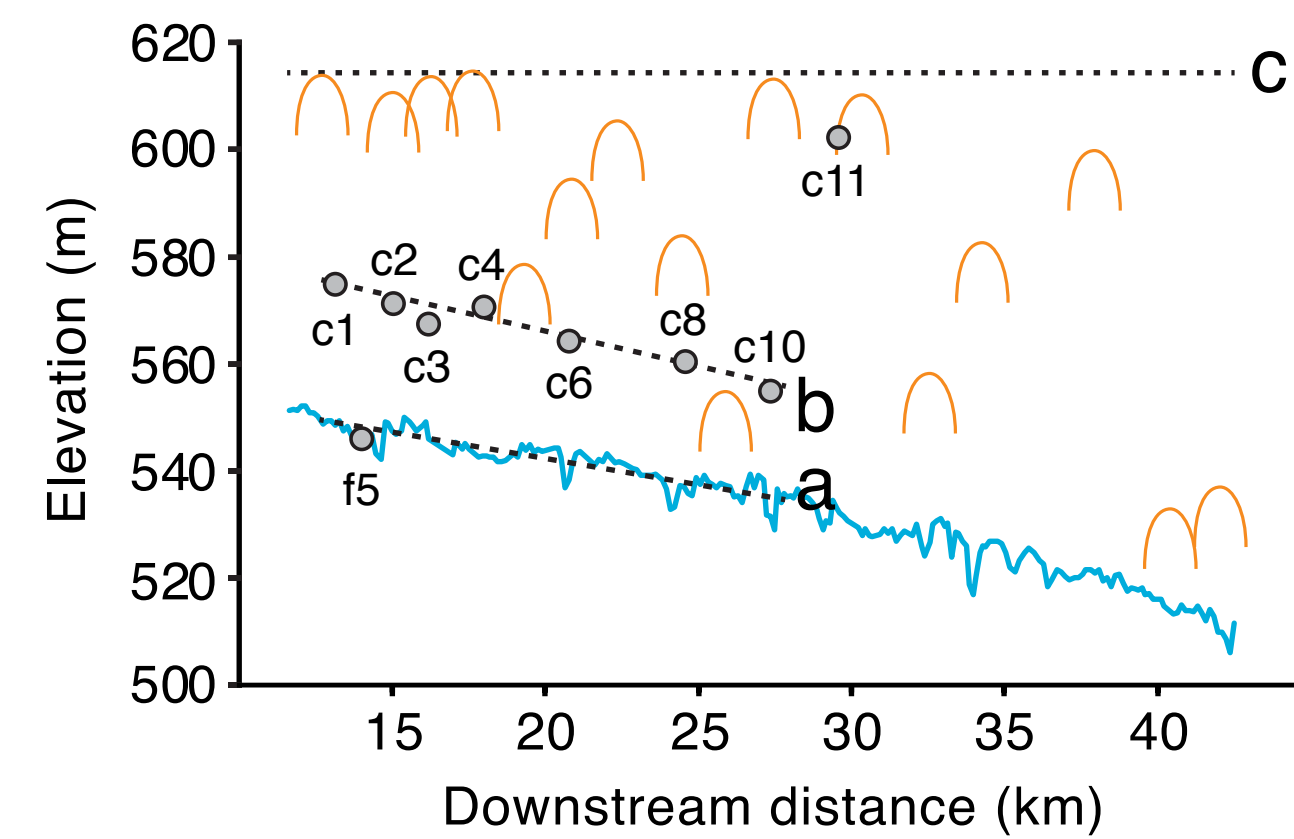


**Fig. 5. Longitudinal river profiles.**

Longitudinal profiles of the Finke gorge channel bed (cyan) relative to the palaeovalley cutoffs sampled for  $^{10}\text{Be}$ - $^{26}\text{Al}$  analysis (grey-filled circles). Note sample c11 is from hilltop fluvial gravels. Average bed slopes (over 95 % confidence intervals) are (a) Finke gorge,  $0.83\text{--}1.02\text{ m km}^{-1}$ , and (b) palaeovalley cutoffs,  $0.85\text{--}1.71\text{ m km}^{-1}$ . The elevation of each bedrock meander core (orange arch) is shown for the 16 cutoffs. A surface (c) fitted to the highest meander cores ( $\sim 614\text{ masl}$ ) defines the estimated minimum level of alluviation. Elevations (in metres above sea level) are based on TOPSAR digital elevation data; distance is measured from the Missionary Plain rangefront.

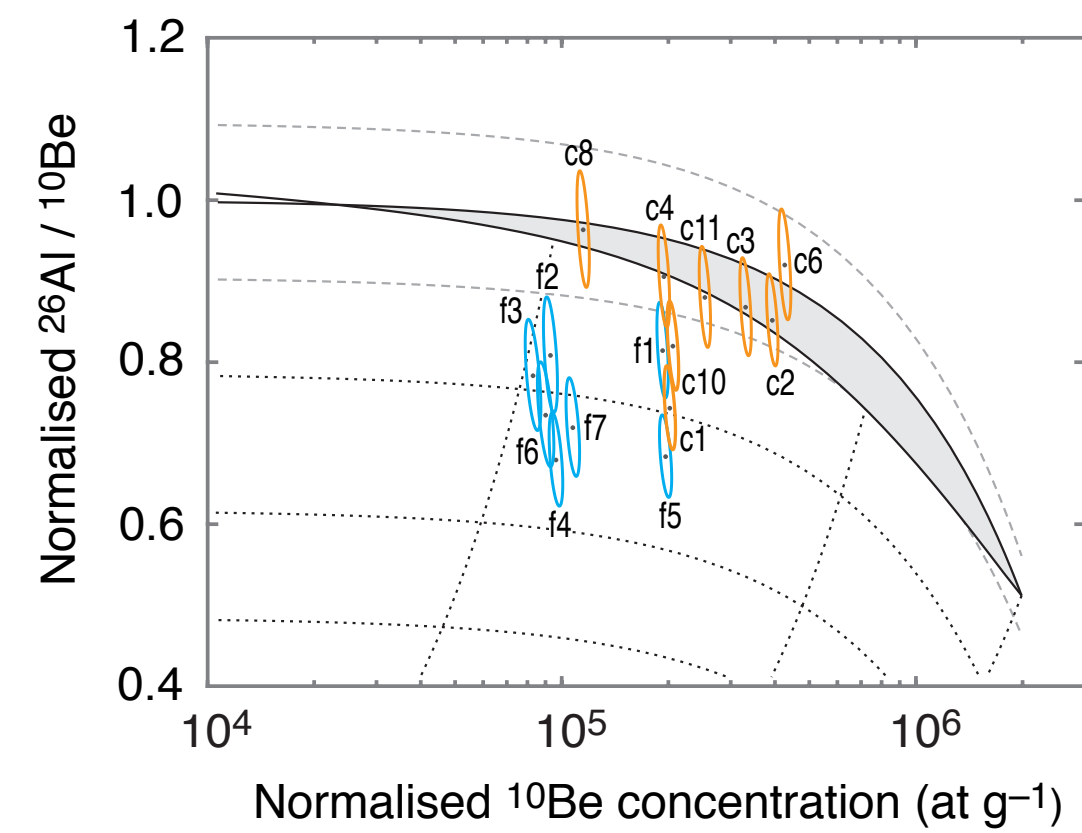


**Fig. 6. Two-nuclide  $^{10}\text{Be}$ - $^{26}\text{Al}$  plot.**

Two-nuclide plot of paired  $^{10}\text{Be}$ - $^{26}\text{Al}$  data normalised to reference production rates for  $^{10}\text{Be}$  ( $4.05 \pm 0.21\text{ at g}^{-1}\text{ y}^{-1}$ ) and  $^{26}\text{Al}$  ( $28.02 \pm 2.25\text{ at g}^{-1}\text{ y}^{-1}$ ), showing  $\pm 1\sigma$  uncertainty in 8 palaeovalley samples (orange ellipses: c1–c11) and 7 channel bed samples (cyan ellipses: f1–f7) upstream, within, and downstream of the gorge. The steady-state erosion island (grey fill) includes  $\pm 1\sigma$  production rate uncertainties (long-dash grey lines). We note that representing  $^{10}\text{Be}$ - $^{26}\text{Al}$  data in a two-nuclide plot assumes steady state exhumation, as in scenario A.

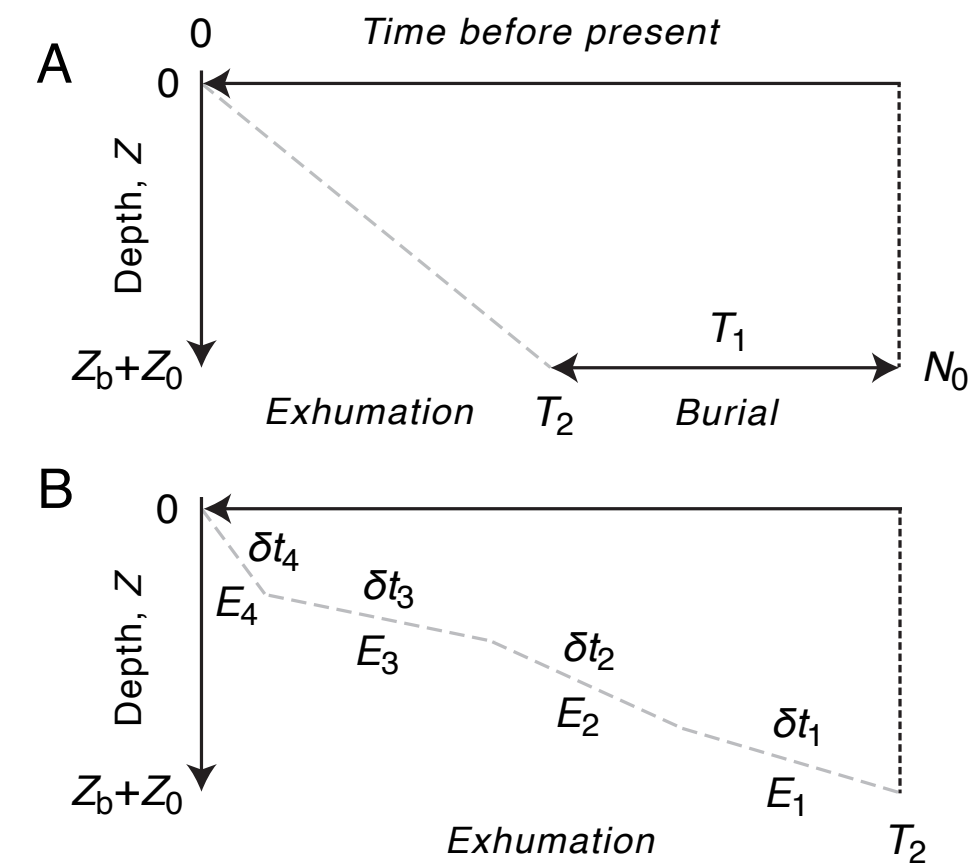


**Fig. 7. Inversion model parameters for scenarios A & B.**

Schematic plots of gravel-pile depth versus time, with the upper-left origin representing the present-day surface, and model parameters: initial concentrations of  $^{10}\text{Be}$  and  $^{26}\text{Al}$ ,  $N_0$ ; period of burial within the gravel-pile,  $T_1$ ; onset of sample exhumation,  $T_2$ , and sample burial depth,  $Z_b + Z_0$ . (A) Gravel-pile depth versus time for scenario A, showing steady exhumation path. (B) Gravel-pile depth versus time for scenario B, showing exhumation paths parameterised with four linear segments of differing exhumation rate ( $E_1$  to  $E_4$ ) over four sequential time intervals ( $\delta t_1$  to  $\delta t_4$ ).

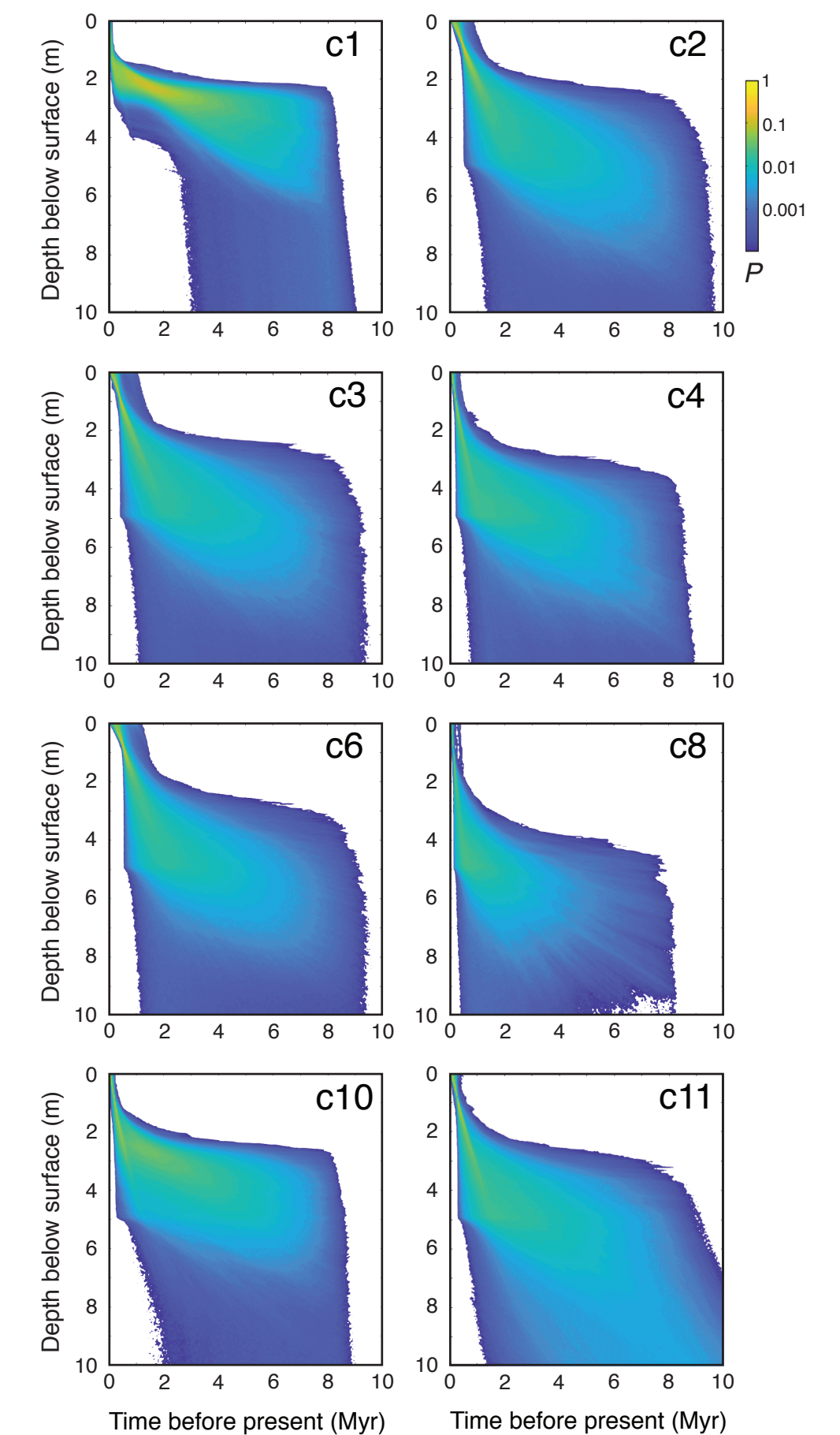


**Fig. 8. Exhumation pathways (scenario B).** Modelled pathways through the upper 10 m of exhumation to the gravel-pile surface;  $P$  is normalised probability density and  $\sim 160,000$  simulations are shown.

# Modelling gravity & surface deflection

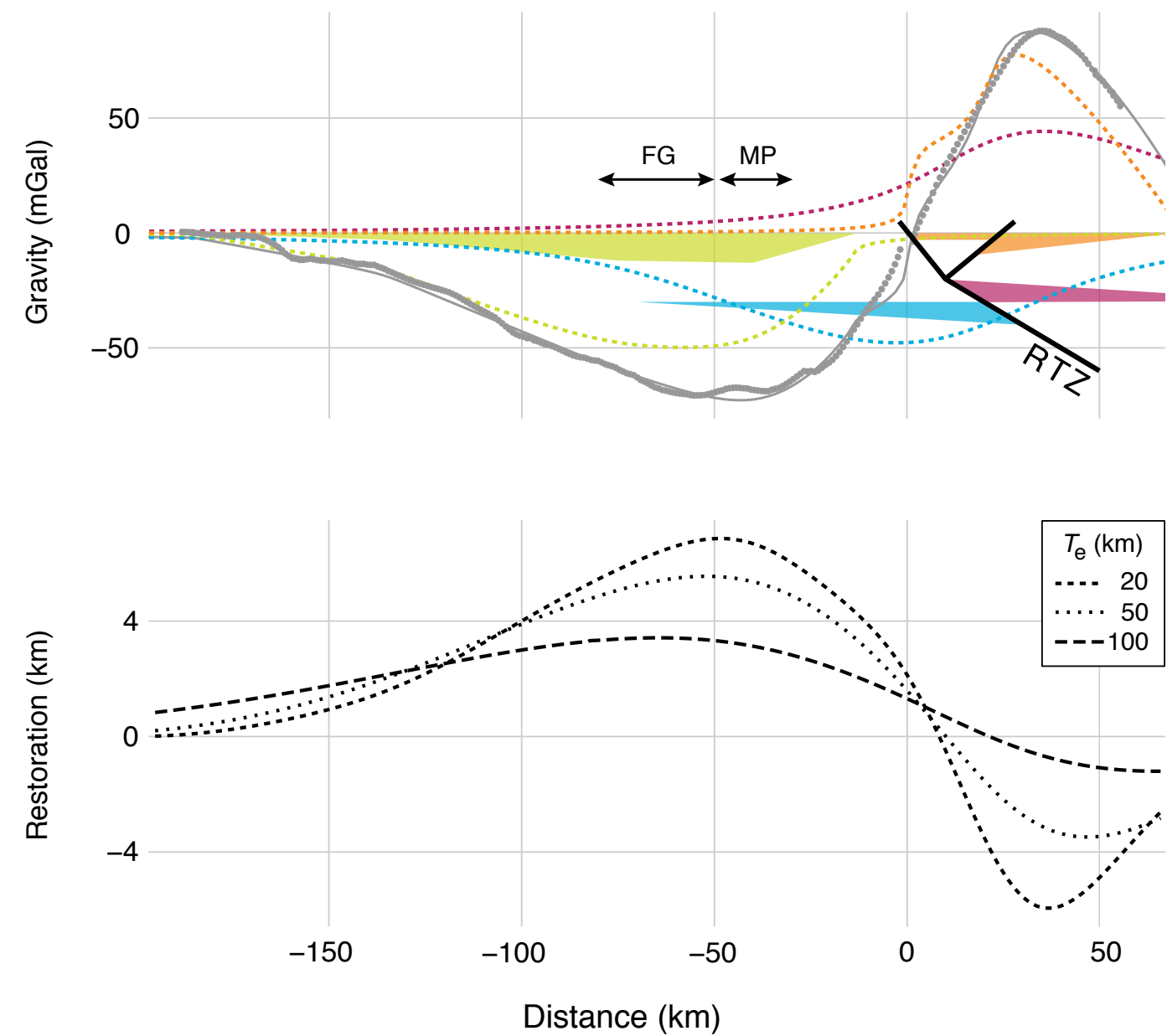


**Fig. 10. Simplified gravity model of the study area.**

(A) Observed and modelled gravity field (grey dots and grey line, respectively) represented as anomalies against a referenced layered crust. Green—footwall foreland basin (density anomaly =  $110 \text{ kg m}^{-3}$ ); cyan—depressed footwall Moho ( $-350 \text{ kg m}^{-3}$ ); plum—elevated hanging wall Moho ( $350 \text{ kg m}^{-3}$ ); orange—elevated hanging wall lower crust ( $310 \text{ kg m}^{-3}$ ), including exposed mafic granulites; RTZ—Redbank Thrust Zone (black line); MP—Missionary Plain; FG—Finke gorge.

(B) Calculated flexural restoration tendency (km) for  $T_e = 100, 50$  and  $20 \text{ km}$ .

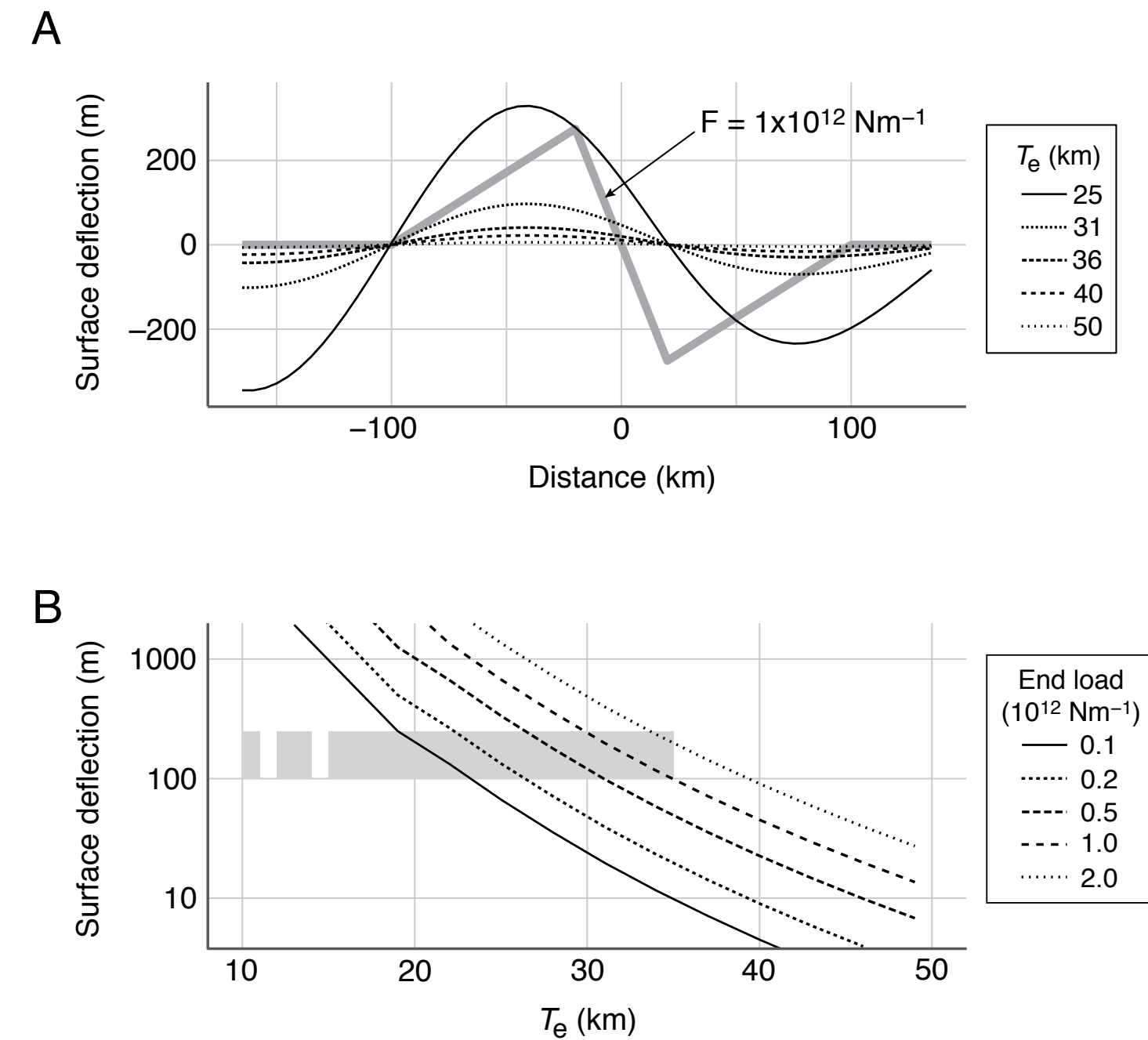


**Fig. 11. Modelled outputs for the elastically supported topographic response to in-plane loads in the presence of embedded loads consistent with central Australia's gravity field.**

(A) Topographic response to an imposed end loading of  $1 \times 10^{12} \text{ N m}^{-1}$  for  $T_e = 25\text{--}50 \text{ km}$  subject to embedded load distribution (thick grey line).

(B) Topographic response as a function of  $T_e$  for different imposed end loads ( $0.1\text{--}2 \times 10^{12} \text{ N m}^{-1}$ ). Thick grey zone shows the plausible range in  $T_e$  assuming the loading results in stress changes of no more than order  $\sim 10 \text{ MPa}$ , with a topographic response of amplitude  $100\text{--}250 \text{ m}$ .

Intertwined bedrock valleys are extremely rare in nonglacial, intraplate settings, and the example in the upper Finke has provided a long-lasting enigma. We propose that the remarkable magnitude of incision and aggradation observed in the Finke is rooted in the geodynamic setting of a Palaeozoic intraplate orogen and the rapid northward migration of the Indo-Australian plate. By combining a MCMC inversion model with cosmogenic  $^{10}\text{Be}$  and  $^{26}\text{Al}$  measurements on palaeovalley gravels in the Finke gorge, we have established that the burial-exhumation in the palaeovalley and associated epigenetic gorge incision occurred over a multi-million-year timescale and likely predates the Quaternary. The nuclide memory in the palaeovalley gravels is decoupled from their source outcrops just  $\sim 50$  km upstream. Aridification over the same timescale appears to have played a secondary role in these events. We suggest that the fluctuating incision-aggradation phases that led to the overprinting of the two bedrock gorges are the product of a combination of short and long-range deformation. The first is a flexural response (at  $\sim 10^2$  km length scales) to extreme uncompensated loads embedded in the crust; the second is rooted in dynamic mantle processes and acts over longer ( $\sim 10^3$  km) wavelengths. The amplitude of topographic responses to inferred variations in end-loading on the plate helps resolve an ongoing debate about the effective elastic thickness of the central Australian lithosphere to no more than 35 km.

## **Acknowledgements**

We thank J. Chappell and P. English for their insightful discussion and G. Pickup for supplying the TOPSAR digital elevation data. The research visit of R.S. Anderson and S.P. Anderson in 2015 was funded by an International Partnership Grant from the University of Wollongong. We acknowledge the Traditional Owners of this Country.